LESSONS LEARNED FROM THE FLIGHT OF THE NASA IN-STEP CRYOSYSTEM EXPERIMENT

Russell S. Sugimura
Jet Propulsion Laboratory
California Institute of Technology
Pasadena, CA 91109 USA
(818) 354-8501

Samuel C. Russo and David C. Gilman
Hughes Aircraft Company
Electro Optical Systems
El Segundo, CA 90245 USA
(310) 616-9651, (310) 616-3813

Abstract

The Cryo System Experiment was developed to validate in near zero-g space a 65 K cryogenic system for focal planes, optics, or other imaging instruments that require continuous cryogenic cooling. Two key cryogenic technologies, designed to improve performance of systems for scientific, commercial and defense applications in space, were successfully demonstrated on NASA's recent shuttle mission, Discovery (STS 63), launched on February 3 - 11, 1995. The two advanced cryogenic technologies consisted of a 2-watt 65 K long-life low-vibration Stirling cooler, and a diode oxygen heat pipe thermal switch. Presented are highlights of the flight experiment and the effectiveness of lessons learned from the system integration of cryocooler and heat pipe technologies relating to: launch-vibration restraints for the expander cold-tips, a high-compliance thermal strap to minimize side loads on the expander, and the value of on-orbit diagnostics to check status of the cryocooler.

INTRODUCTION

The Cryo System Experiment (CSE) achieved its objectives, demonstrating, the ruggedness to withstand the space shuttle launch vibrations, and characterizing the performance of two thermal management technologies: a Hughes 2-watt 65 K long-life low vibration Stirling cycle. Improved Standard Spacecraft Cryocooler (ISSC), and a Hughes experimental diode oxygen heat pipe that enables large physical separation between the cryocooler and a thermal load, and also provides on-off switching to limit reverse heat flow when the cooler is turned off. In addition to the flight performance data (Hughes 1995), an important result of the experiment was the establishment of flight-heritage data that thoroughly demonstrates the system's flight qualification status and compliance with launch vehicle safety and cryosystem integration constraints.

The ISSC, which provided >1.2. watts of cooling at 60 K during the flight experiment, is an improved version of the 65 K Standard Spacecraft Cryocooler (SSC) developed by Hughes under Air Force Phillips Laboratory/Ballistic Missiles Defense Office (AFPL/BMDO) sponsorship. The ISSC consists of a compressor connected to an expander by a transfer tube and the control electronics. It is the first U.S.-built long-life Stirling cooler to operate in space. Its continuous performance over the course of the eight-day mission equaled its performance during ground testing. 'l'he experiment was complemented by a ground-based life-test program, funded by the DoD. At this time two ISSC life-test coolers have each demonstrated over two years of continuous operating time; the life teats are ongoing and are anticipated to continue for the next several years.

The second cryogenic component successfully demonstrated was a diode oxygen heat pipe. The diode oxygen heat pipe is designed to provide a high-conductance path between the cryogenic load and the cryocooler, when operating in the "forward mode." The diode nature of the heat pipe limits heat conduction in the reverse direction ("reverse-mode" operation) when the cooler is turned off.

Prior to the CSE flight experiment, diode oxygen heat pipe characterization testing was limited to laboratory vacuum chambers. Due to the poor capillary pumping capability of oxygen, there had been serious concern that one-g testing was optimistically influenced by puddle flow. A key objective of the CSE was to generate a zero-g test database to resolve this issue. The shuttle based experiment resolved a key technical concern by demonstrating that the diode. oxygen heat pipe does work in the near-zero gravity of space..

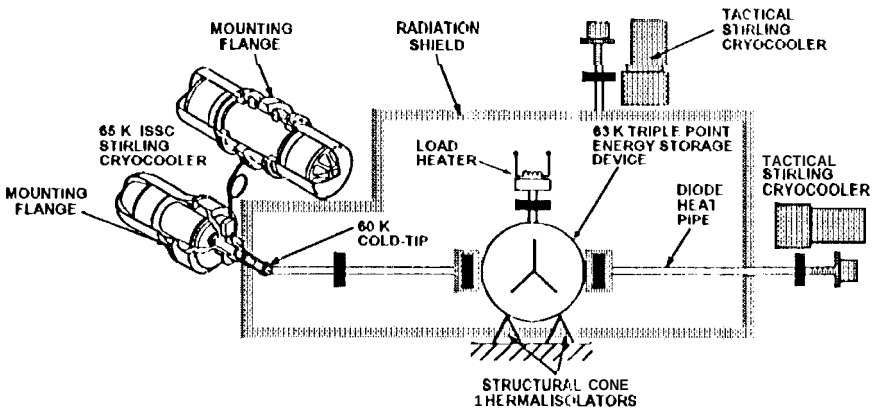

FIGURE 1. Cryo System Experiment Mechanical Subsystem Block Diagram.

In addition to the ISSC described above, a second type of cryocooler was used. 'J'his rotary drive, tactical piston-driven Stirling cooler was designed by Hughes to have a relatively large cooling capacity and an anticipated life on the order of 1000 hours. This cooler has successfully flown on previous shuttle flight experiments to support a rapid cooldown, allowing more time for the actual experiment to be performed at cryogenic temper-at ure. Its predecessors have been used 10 cool sensors in aircraft and missiles where mechanical robustness and insensit ivit y to vibrat ion are key requirements.

Figure 1 is a block diagram of the CSE with the ISSC connected to the simulated triple-point (TRP) mass through a thermal heat strap. One tactical cooler is connected through the diode oxygen heat pipe to the opposite side of the simulated TRP. This physical arrangement was selected to reduce risk should a failure occur within the heat pipe or the ISSC. In an operational system the diode oxygen heat pipe would be located between the ISSC and the thermal energy storage device,. A second tactical cooler was used to minimize parasitic by cooling a radiation shield to a temperat ure of 130 K. In a non-shuttle flight system, shield cooling is generally provided by a cryogenic radiator.

LESSONS LEARNED

An important thrust of the. CSE was the integral ion of the cryocoolers into this cryogenic system. As long-life, low-vibration cryocoolers transition from an emerging to an enabling technology, the focus shifts from cooler performance. issues (volume, mass, thermal, input/output power, electrical) to system compatibility and integrat ion issues. 'J'he. following paragraphs summarize the results of the lessons learned (Sugimura 1995) dur ing the system integration phase of this shut tle-flight experiment.

Launch Vibration

A key challenge was to resolve the issue of launch vibration and the impact to the cryocooler expanders. The expander cold finger, a relatively thin-wall, hollow tube in which the expander piston shuttles, is necessarily thin to minimize parasitic thermal loads due to axial heat transfer. Although by itself the expander coldfinger may be considered relatively robust, it is necessary to include a thermal transfer path to provide, cooling to the load. This is accomplished by an interface between the. expander cold-tip (usually a copper Mock) and a flexible the.rmd strap to provide a path to the thermal load. The supported interface masses at the cold-tip for the ISSC totaled 2S0 gm (0.55 lb) and for the tactical coolers totaled 164 gm (O. 36 lb).

'J'he sizable interface masses attached to the cold finger tip can crest,. a significant dynamic load on the. expander cold finger during launch. To prevent damage due to the launch vibrations, all three of the cryocooler were fitted with constraint mechanisms designed to limit cold finger movement. The CSE vibration const mint designs consist of two different G-1O fiberglass configurations: one for the ISSC, and one for the. two tactical cryocoolers. Subsequent to assembly, the system was vibrated to proto-flight qualification levels without incident. Post-flight experiment disassembly revealed that both G-10 fiberglass constraint designs proved adequate to protect the cryocooler expanders from launch vibration damage, as well as from landing impact and transport vibration damage.

TABLE 1. Predicted Cold-Tip Loads for the Original and Modified Thermal Strep Designs.

Load	Original (lb)	Modified (lb)
Vacuum induced lid load - 0.012" cold-tip movement	0.25	0.12
Thermal contraction load -0.020" contraction of TRP	0.43	0.20
Total anticipated Loads	0.68	0.32
Unanticipated mechanical integration load - Preload	>1.1	0.51
Total Load	>1.78	0.83
Margin @1.4 lb, max. acceptable load	-21%	40%

High-Compliance Thermal Strap

Design of the thermal strap connecting the ISSC cold-tip to the cryogenic load was carefully considered to optimize two conflicting critical characteristics of the strap: thermal conductance and mechanical stiffness. It is desirable that the conductance be high (>0.5 W/K) due to the strong dependence of cooler efficiency on cold-tip temperature, and that the spring rate be low due to the sensitivity of the expander cold finger to mechanical side loads.

Table 1 summarizes the predicted cold-tip loads for each of the contributive forces for both the original and modified thermal strap designs. The "unanticipated loads" are the result of unavoidable, but small alignment errors introduced when mechanically integrating the. thermal strap into the system. The lesson learned is that this-load must be allowed for when specifying the acceptable thermal strap spring rote. "l"he conclusion was that the 1.78 lbs maximum side load imposed on the expander cold-tip by the original thermal strep was too large. It was shown that due to the close tolerances within the ISSC, the total combination of forces from the thermal strap preload, thermal contraction loads and the additional force created by the canister lid deflection, was sufficient to cause contact. The goal was to increase the mechanical compliance at the expense of somewhat lower thermal conductance, and thereby to reduce the side-load force imposed on the cold finger.

The original design provided a thermal resistance of 0.5 K/W and consisted of 39 layers of 0.004" x 1.5" of OFHC copper, giving a total cross-sectional area of 0.234 in^2. The layers at each end of the strap were soldered together. The design concept after modifications, Fig. 2, resulted in a thermal resistance of 1.1 K/W and had 34 layers of 0.004" x 0. 8" of OFHC copper; the resulting total cross-sectional area is 0.109 in^2.

Figure 2 shows the modified thermal strap design and identifies the reference axes used in Table 2, a comparison between the measured thermal strap spring rates for the original and modified designs. There was no contact between the displacer and cold cylinder sidewall after installation of the strap, or after attaching the upper end plate and establishing vacuum conditions within the canister. The mechanical system was vibrated to protot ype flight qualification levels, subjected to thermal-vacuum test, and successfull y completed the. flight experiment without incident.

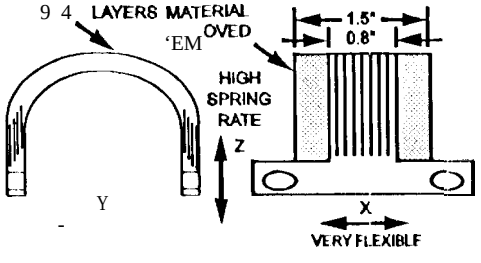

FIGURE 2. Modified Design and References Axes.

TABLE 2. Measured Thermal Strap Spring Rate for the Original, and Modified Designs.

Axis	Original free-free (lb/in)	Modified free-free (lb/in)
X	N/A	1.4
Y	4.0	1.6
Z	11.9	4.2

FLIGHT EXPERIMENT HIGHLIGHTS.

'l'he flight experiment timeline was identical to the ground test timeline used in the pre-flight thermal-vacuum qualification test, and consisted of five phases: (1) ground hold, launch and system checkout, (2) on-orbit cooldown, (3) main flight experiment, (4) extended flight experiment and (5) post-experiment shutdown. The main flight experiment consisted of three cycles of heat pipe tests at 63.5 K and the ISSC test at a nominal 60 K. The extended experiment consisted of an additional heat pipe test series at 80 K (three cycles) and continued ISSC testing. The main experiment temperature responses for the ISSC, heat pipe and RS cryocoolers are shown in Fig. 3, with Mission Elapsed Time (MET) as a function of temperature.

Diode Oxygen Heat Pipe Tests

During steady-state conditions, at nominal operating temperatures of either 63.5 K or 80 K, the forward-mode heat pipe conductance, $G_{Forward}$, was:

$$0.54 \text{ W/K} \leq G_{Forward} \geq 0.66 \text{ W/K at 63.5 K, and}$$
$$0.88 \text{ W/K} \leq G_{Forward} \geq 1.08 \text{ W/K at 80 K.}$$

The results of the heat transport test demonstrated that the heat pipe can transport the 1.95 watt of heat load with the overall temperature drop from condenser to evaporator limited to 2.95K. The flight test results showed a slight improvement of heat pipe performance over ground test results obtained during heat pipe qualification tests at both 63,5 K and 80 K, Table 3. These results arc cent rary to heat pipe community expectations, and further study and evaluation of the flight test data arc required before this result is fully understood.

Heat pipe flight test performance, as summarized in q'able 3, is comparable with thermal-vacuum ground test results for reverse-mode conductance and start-up and shut-down t ransition t i mes. Reverse-mode conductance was demonstrated with the evaporator being maintained at essentially the same temperature as in the forward mode. whi le increasing the condenser temperat ure until there was a t emperat ure di fference of 80K or greater bet ween the two regions of the heat pipe. (Fig. 3).

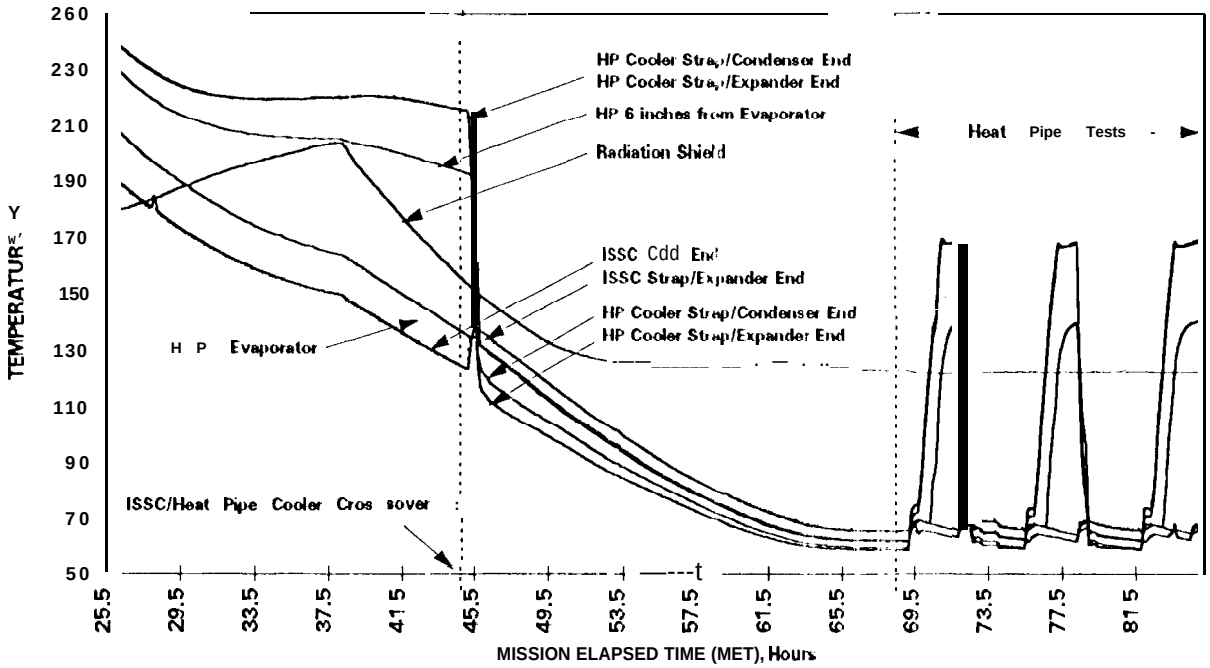

FIGURE 3. Cryo System Experiment -1 leat Pipe Experiment Tests.

TABLE 3. Comparison of Heat Pipe. Flight and Ground Test Results.

Experiment Phase	Test Description	Performance Goal DesignPoint Performance	$Q_{load}=(T6-T8)*C_{strap}$ W		ΔT_{HP} (T1+T2)/2-T5 K		Elapsed Transition Time-hrs		Calculated Conductance W/K	
			Flight Test	Ground Test	Flight Test	Ground Test	Flight Test	Ground Test	Flight Test	Ground Test
	Start-up	(T1+T2)/2 - T5's < 3K								
Baseline Test (63.5 K)	Cycle 1				2.33	3.09	N/A	N/A		
	Cycle 2				2.99	2.74	0,70	.53		
	Cycle 3				3.34	3,74	.70	.50		
Extended Test (80K)	cycle 4				1.51	1.8	N/A	N/A		
	Cycle 5				1.40	1.38	0.51	0.53		
	Forward Mode Conductance	$Q_{load}/\Delta T_{HP}>1$ W/K								
Baseline Test (63.5 K)	Cycle 1		1.53	1.75	2.36	3.08			.65	0,57-
	Cycle 2		1.95	1.76	2.95	3.06			0.66	0,57
	Cycle 3		1.50	1.38 1.38	2.79	4.3]			0.54	0,32
Extended Test (80K)	Cycle 4		1.47	1.43 1.43	1.61	1.86			0.88	0.77
	Cycle 5		1.43	1.71	1.33	2.07			1.08	0.83
	Shutdown	Transition <1 hour								
Baseline Test (63.5 K)	Cycle 1				-74.51*	-95.9*	1.0	1.0		
	Cycle 2				-108.23	-98.5	1.0	.86		
Extended Test (80K)	Cycle 4				-98.45	-82.7*	1.0	1.0		
	Cycle 5				-98.35	-93.1	1.0	1.0		
	Reverse Mode Conductance	T5 - (T1 + T2)/2 > 80 K								
Baseline Test (63.5 K)	Cycle 1		1.07	1.0	-102.19	-100.0			0.01	0.01
	Cycle 2		1.1	0.861	-108.11	-100.43			0.008	0.008
Extended Test (80K)	Cycle 4		0.94	1.0	-98.35	88.39			0.01	0.011

ΔT_{HP} = Heat Pi Temperature Difference; Q_{LOAD} = Heat Pipe Transport Capacity; C_{STRAP} = Heat Pipe Thermal Strap Conductance; and
S*ΔT_{HP}@End Transition Time.

During steady-slate condit ions, at nominal operating temperatures of either 63. SK or 80K, the reverse-mode heat pipe conductance , $G_{Reverse}$, is in good agreement with ground test data (Table 3):

$$0.008 \text{ W/K} \leq G_{Reverse} \geq 0.01 \text{ W/K}$$ at both 63.5 K and 80 K.

The time **required to complete** heat **pipe start-up was approximately** 40 minutes, and was consistent with subsequent start-up t imes during recovery from successive 60 K reverse-mode basel ine heat pipe tests, and from the extended 80 K tests as well. Observed flight and ground test startup performance results were essentially the same, and recorded startup times were both on the order of 30 - 40 minutes. The data base is sufficient to establish if start-up is limited by the thermal mass of the TRP or the heat pipe dynamics. Further study and evaluat ion of the data arc required to fully assess the fluid dynamic behavior.

The observed shutdown times were approximately one hour for all cycles at both 63.5 K and 80 K, These times are in good agreement with the ground test results, as shown in Table 3.

Additionally, due to an unexpected test result in which the diode heat pipe once failed to easily turn off, further tests were conducted. These additional tests confirmed that the radiation shield (RS) cooler vibration level, which is much higher than the ISSC vibration level, apparently acts to enhance wicking in the heat pipe, thereby making

it more difficult to shut clown the pipe. 'I'his is an important heretofore unobserved zero-g effect that has be-en postulated by Jones and Wu (Jones 1995) to possibly be due to the Coanda boundary layer effect (Lachmann 196 1). Curiously, vibrat ion of heat pipes in a one-g field has been shown to actually deter performance (Huber 1993), possibly due to the fact that gravity may force the wick fluid to fall out when vibrated. Additional study of the data is required to fully assess the implications of this effect for space use of both diode heat pipes and conventional heat pipes.

ISSC Test

The test objectives were to demonstrate startup and cooldown and generate a data base for comparison with ISSC performance documented during thermal-vacuum ground test, Dur ing periods of steady-state operation the ISSC demonst rated cooling capacity > 1.2W al 60 K, with a heat rejection temperatur e at the cryocooler mounting surfaces ranging from 300 K to 310 K. Both 1 SSC flight test transient performance data during cooldown and ISSC steady-slate flight test performance at 60 K and at 80 K were comparable to ground test transient thermal-vacuum performance data.

The ISSC was designed with very c1o.sc tolerance, non-contacting, metal-to-metal surfaces between the expander piston and its cylindrical cold finger sidewall. Included in the design is an electrical resistance measuring circuit that indicates any momentary or prolonged contact between the expander piston and its cylinder sidewall, or its end stops. This circuit has proved essential in a number of diagnostic situations during both the system integration process and the flight experiment,

For example, during the. quick functional test, the ISSC expander piston was stroked to verify operation prior to starting the flight experiment cooldown timeline. Full piston stroke was achieved with no contact indicating that the cryocooler piston was properly aligned and that the cold finger did not have excessive side loads imposed on it by the thermal strap, resulting in a high level of confidence. that the cryocooler had been unaffected by launch vibrations.

'l'he cooler compressor and expander designs incorporate the capability to use the position of the piston as a function of drive current to obtain a plot of the hysteresis or drag of the pistons against the. cylinder side. wall. 'l'his circuit was used extensive] y throughout the flight experiment to validate, cooler clearances, and during both cryocooler and heat pipe flight experiments with no indication of piston/cylinder contact. This validation is the only means to confirm that the compressor piston suspension system is operating sat isfactoril y following system integrat ion and qualificat ion tests.

During the extended flight experiment interval a series of steady-state cooling load points were obtained as a function of load temperature with lSSC motor power as a parameter. The result i ng, flight load and power curve is presented in Figure 4, relative to ground test data, ISSC performance (cooling capacity vs. load temperature) increased slightly in flight results relative to ground results. Post -flight tests of the 1 SSC performed at GSFC and at Hughes showed no difference between pre-flight ground pet formance and post-flight ground performance.

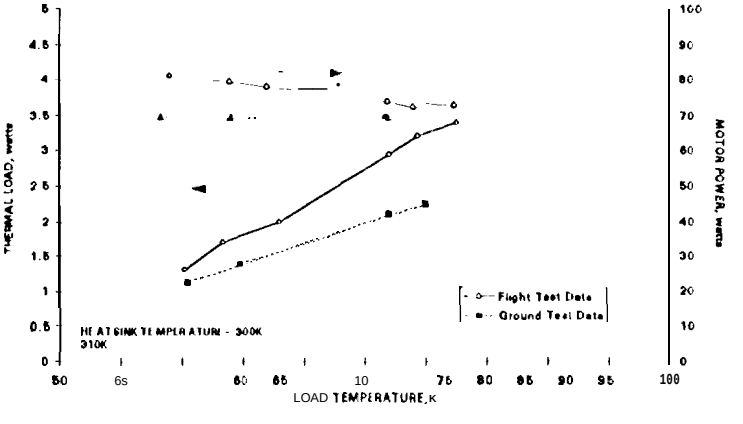

FIGURE 4. CSE lSSC Flight and Ground Test Load Curves

SUMMARY

The eight-day flight experiment enabled CSE to validate the zero-g operation of a Hughes ISSC, and a Hughes diode oxygen heat pipe thermal switch. Both CSE thermal management technologies are strong candidate for use in future NASA (i.e., Earth Observing System) and DoD (Space Missiles and Tracking Systems, formerly Brilliant Eyes) cryogenic subsystems associated with precision space-science instruments being designed for 5- to 10-year lifetimes. The CSE illustrates an important type of NASA space flight experiment in which enabling technologies are validated to provide the option for subsequent application in near-future space system developments .

The CSE successfully completed all mission objectives, and far exceeded expectations in term of the test apparatus performance and in the wealth of micro-gravity data obtained. These results are available for study by the heat pipe and cryocooler community, yielding new insights into the thermal and fluid dynamic behavior of heat pipes operating in zero-g and into the robustness and zero-g performance of Stirling cycle cryocoolers.

Acknowledgments

The work de.scribed in this paper *was carried* out by Hughes Aircraft Company, Electro Optical Systems, under Contract #958996 with the Jet Propulsion Laboratory, California Institute of Technology, sponsored by the National Aeronautics and Space Administration.

Particular credit is due M. Barr, G. Fleischman, D. Gilman, Y. Lin, R. McVey, P. Mayner, G. Pavlina, T. Pollock, K Price, S. Solosky, B. Wolf, and A. Wong of Hughes, and J. Jones and R. Ross, Jr. of JPL, whose dedication and diligence in identifying and resolving the issues and challenges are deeply appreciated.

References

Huber, N. F., (1993) "Effect of Longitudinal Vibration on the Capillary Limit of a Wrapped Screen Wick Copper/Water Heat Pipe, " M.S. Thesis, Air Force Institute of Technology, Wright-Patterson AFB, OH, Rept #AD-A273830 AFIT/GAE/ENY/93D-18.

Hughes Aircraft Company (RUSSO, S. C.), "Final Report - Cryo System Experiment, " In Publication.

Jones, J. A. and Wu, J. J., (1995) Thermal Sciences and Cryogenics Group Jet Propulsion Laboratory, California Institute of Technology, Pasadena, CA, Private Communication.

Newman, B. G., (1961) "The Deflexion of Plane Jets by Adjacent Boundaries - Coanda Effect," *Boundary Layer and Flow Control,* Volume 1, Edited by G. V. Lachmann, Pergamon Press, New York, 232-264.

Sugimura, R. S., Russo, S. C., and Gilman, D. C., (1995) "Lessons Learned during the Integration Phase of the NASA IN-STEP Cryo System Experiment," *Cryocoolers* 8, Edited by R. G. Ross, Jr., Plenum Press, New York, 869-882.